Research Article | Vol. 24, No. 24 | 28 Nov 2016 | OPTICS EXPRESS 27104

Optics EXPRESS

Highly alignment tolerant and high-sensitivity 100Gb/s (4 × 25Gb/s) APD-ROSA with a thin-film filter-based de-multiplexer

JOON YOUNG HUH, SAE-KYOUNG KANG, JIE HYUN LEE, JOON KI LEE, AND SUNME KIM

Electronics and Telecommunications Research Institute (ETRI), 218 Gajeong-ro, Yuseong-gu, Daejeon, 305-700, South Korea

*yurinara@etri.re.kr

Abstract: We investigate and demonstrate a 100-Gb/s (4x25-Gb/s) receiver optical sub-assembly (ROSA) based on avalanche photodiodes and a thin-film filter-based de-multiplexer. The overall alignment tolerances of the ROSA are relaxed to have larger than ± 25 μm by improving optical coupling structure. The receiver sensitivity of each lane is also measured to be less than –22.2 dBm, a record minimum to our knowledge, at the bit error ratio of 10^{-12} for 25.78-Gb/s NRZ signal.

OCIS codes: (060.2330) Fiber optics communications; (220.1140) Alignment; (250.5300) Photonic integrated circuits.

References and links

1. IEEE Standard 802.3ba, "40Gb/s and 100Gb/s Ethernet task force," *http://www.ieee802.org/3/ba/*.
2. IEEE Standard 802.3bs, "200 Gb/s and 400 Gb/s Ethernet task force," *http://www.ieee802.org/3/bs/*.
3. M. Nada, T. Yoshimatsu, Y. Muramoto, H. Yokoyama, and H. Matsuzaki, "Design and performance of high-speed avalanche photodiodes for 100-Gb/s systems and beyond," J. Lightwave Technol. **33**(5), 984–990 (2015).
4. Y. Doi, M. Oguma, T. Yoshimatsu, T. Ohno, I. Ogawa, E. Yoshida, T. Hashimoto, and H. Sanjo, "Compact high-responsivity receiver optical subassembly with a multimode-output-arrayed waveguide grating for 100-Gb/s Ethernet," J. Lightwave Technol. **33**(15), 3286–3292 (2015).
5. N. Keil, H. H. Yao, C. Zawadzki, W. Schlaak, M. Möhrle, and N. Grote, "Polymer optical motherboard technology," in *Proceedings of European Conference on Integrated Optics* (2007), paper ThD2.
6. B. Pezeshki, J. Heanue, D. Ton, T. Schrans, S. Rangarajan, S. Zou, G. W. Yoffe, A. Liu, M. Sherback, J. Kubicky, and P. Ludwig, "High performance MEMS-based micro-optic assembly for multi-lane transceivers," J. Lightwave Technol. **32**(16), 2796–2799 (2014).
7. J. K. Lee, J. Y. Huh, S.-K. Kang, and Y.-S. Jang, "Analysis of dimensional tolerance for an optical demultiplexer of a highly alignment tolerant 4 × 25 Gb/s ROSA module," Opt. Express **22**(4), 4307–4315 (2014).
8. G. E. Tangdiongga, T. G. Lim, J. Li, C. W. Tan, P. V. Ramana, Y. Y. Chai, S. Maruo, and J. H.-S. Lau, "Optical design of 4-channel TOSA/ROSA for CWDM applications," Proc. SPIE **6899**, 68990I (2008).
9. H. Aruga, K. Mochizuki, H. Itamoto, R. Takemura, K. Yamagishi, M. Nakaji, and A. Sugitatsu, "Four-channel 25Gbps optical receiver for 100Gbps Ethernet with built-in demultiplexer optics," in *Proceedings of European Conference on Optical Communication* (2010), paper Th.10.D.4.
10. Y. Fujimura and F. Nakajima, "Receiver optical module for receiving wavelength multiplexed optical signal," United States patent 14/0346323 (November 27, 2014).
11. CFP multi-source agreement, "CFP4 hardware specification revision 1.1," (2015), *http://www.cfp-msa.org/Documents/CFP-MSA_CFP4_HW-Spec-rev1.1.pdf*.
12. S. F. F. Committee, "QSFP+ 28 Gb/s 4X pluggable transceiver solution (QSFP28)," (2015), *ftp://ftp.seagate.com/sff/SFF-8665.PDF*.
13. S.-K. Kang, J. K. Lee, J. Y. Huh, J. H. Lee, and S. M. Kim, "Receptacle collimator and multi-wavelength optical receiving module including the same," United States patent 15/010657 (January 29, 2016).
14. J. K. Lee, S.-K. Kang, J. Y. Huh, K. Kim, and J. Lee, "Multi-wavelength optical signal receiving apparatus and method," United States patent 9360641 (June 7, 2016).
15. T. Murao, N. Yasui, K. Mochizuki, M. Shimono, H. Kodera, D. Morita, T. Yamatoya, and H. Aruga, "Lens alignment technique using high-power laser for hybrid integrated multi-channel transmitter optical sub-assemblies," IEEE Photonics Technol. Lett. **25**(20), 1958–1960 (2013).
16. T. Ohyama, Y. Doi, W. Kobayashi, S. Kanazawa, T. Tanaka, K. Takahata, A. Kanda, T. Kurosaki, T. Ohno, H. Sanjoh, and T. Hashimoto, "Compact hybrid-integrated 100-Gb/s TOSA using EADFB laser array and AWG multiplexer," IEEE Photonics Technol. Lett. **28**(7), 802–805 (2016).

#276446 http://dx.doi.org/10.1364/OE.24.027104
Journal © 2016 Received 30 Sep 2016; revised 27 Oct 2016; accepted 8 Nov 2016; published 14 Nov 2016

Optics EXPRESS

17. S.-K. Kang, J. K. Lee, J. Y. Huh, J. C. Lee, K. Kim, and J. Lee, "A cost-effective 40-Gb/s ROSA module employing compact TO-CAN package," ETRI J. **35**(1), 1–6 (2013).
18. M. Huang, P. Cai, S. Li, L. Wang, T. Su, L. Zhao, W. Chen, C. Hong, and D. Pan, "Breakthrough of 25Gb/s germanium on silicon avalanche photodiode," in *Proceedings of Optical Fiber Communication Conference* (Optical Society of America, 2016), paper Tu2D.2.

1. Introduction

With the rapid increase of bandwidth-consuming applications such as smart devices, social networking, cloud computing and on-line streaming, the internet data traffic grows explosively. To accommodate ever-increasing traffic data, the 40G/100G Ethernet was standardized in 2010 [1]. The standardization of 200G/400G Ethernet is currently underway and it is planned to be completed in 2017 [2]. In Ethernet standards, wavelength-division multiplexing (WDM) technology is being widely adopted to cope with the transmission capacity. For the WDM technology, an optical de-multiplexer (DMUX) is necessary to separate many optical signals having different wavelengths in the receiver. In order to overcome the limited space in datacenters using Ethernet, there have been many efforts to integrate the optical DMUX into a receiver optical sub-assembly (ROSA) [3–14]. The DMUX has practically been implemented by two types: one is a planar light-wave circuit (PLC) based arrayed waveguide grating (AWG), and the other is a thin-film filter (TFF) based DMUX. The former has been applied in various optical components because of the high productivity and scalability [3–6, 15, 16]. However, it has a stringent alignment tolerance such as a few micrometers and slightly high insertion loss, because of the small waveguide size [4–6]. On the other hand, the latter provides large alignment tolerance and very low insertion loss [7–10]. For this reason, the TFF-based DMUX can become an attractive solution for extending the transmission distance.

In this paper, we investigate and demonstrate the performance of 100-Gb/s (4 × 25-Gb/s) ROSA based on avalanche photodiodes (APDs). In order to achieve large alignment tolerance and high receiver sensitivity, the TFF-based DMUX has been integrated into the ROSA instead of the PLC-based AWG. The fabricated ROSA is composed of a receptacle including a collimating lens, a TFF-based DMUX and an APD block, which is composed of four APDs, 4-channel array trans-impedance amplifier (TIA) and a focusing lens. It is compact enough for CFP4 and QSFP28 form-factors [11, 12]. In order to achieve the best performance, it is necessary to fully look into the optical coupling and alignment tolerance among the key components such as a receptacle, a TFF-based DMUX, and an APD block. Previously we have only analyzed the dimensional error of the TFF-based DMUX for the ROSA [7]. This paper first provides the detailed investigation regarding the coupling efficiencies and alignment tolerances of the collimating lens and the focusing lens in the receptacle and the APD block, respectively. For the efficient fabrication, we also examine the alignment tolerances among the receptacle, the TFF-based DMUX and the APD block in the ROSA. It is reported that the overall alignment tolerances of the ROSA with the TFF-based DMUX are larger than the PLC-based AWG. From these investigations, we have properly assembled the key components to maximize the performance of the ROSA. As a result, the receiver sensitivity of the ROSA has been measured to be the best sensitivity to our knowledge. We have also succeeded in error-free transmission of 4 × 25-Gb/s signal on the 60-km standard single mode fiber (SSMF) without an optical amplifier.

2. Design and Structure of 4 × 25-Gb/s APD-ROSA

Figure 1(a) shows the block diagram of the 4 × 25-Gb/s APD-ROSA. In order to achieve the large tolerance and good performance of the ROSA, a TFF-based DMUX has been applied and optical coupling structure has been improved in the ROSA. The DMUX separates the optical input signals of four wavelengths into four APDs. The center wavelengths of four lanes in the DMUX are 1295.56 nm, 1300.05 nm, 1304.58 nm, and 1309.14 nm, which are in the wavelength standard of the local area network – wavelength division multiplexing (LAN-

Optics EXPRESS

WDM) [1]. Figure 1(b) shows the proposed structure of the ROSA, which is composed of a receptacle, a TFF-based DMUX and an APD block. The receptacle having within a collimating lens has been proposed for the efficient collimation of the input optical signal launched from the SSMF [13]. The focusing length and multiplication factor of the glass-based collimating lens have been designed to be 700 μm and infinity, respectively.

Figure 1(c) shows the schematic diagram of the TFF-based DMUX using the zigzag multi-reflection scheme [7]. The TFF-based DMUX consists of a parallelogram-shaped optic block and four LAN-WDM TFFs. The anti-reflection (AR) coating is applied on the input and output regions of the TFF-based DMUX. And the high-reflection (HR) coating is incorporated into the opposite side of the TFFs in the optic block. The angle of incident (AOI) of each TFF is 8°. The width of each TFF is 500 μm, because the pitch of four lanes has been designed to be 500 μm. The length of each TFF is 750 μm. The length of optic block has been designed to be 2.7 mm.

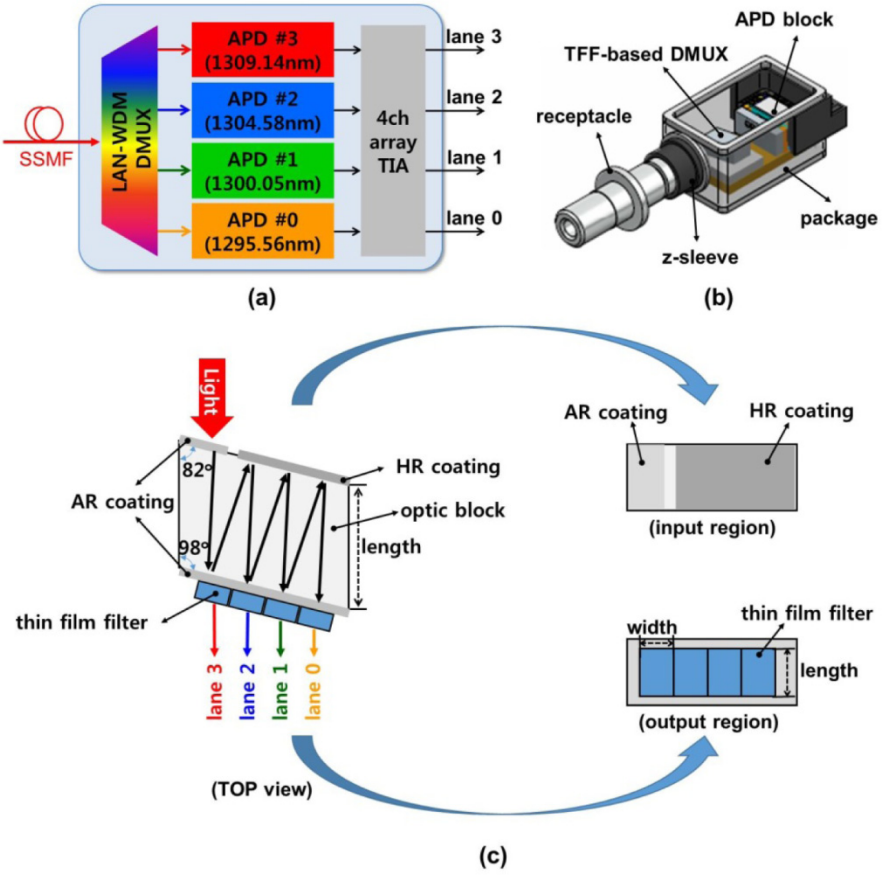

Fig. 1. (a) Block diagram of the 4 × 25-Gbps APD-ROSA. (b) Proposed Structure of 4 × 25-Gb/s APD-ROSA. (c) Schematic diagram of a TFF-based DMUX.

The APD block consists of four APDs, a 4-channel array TIA and a focusing lens. The focusing lens is the array lens to simultaneously concentrate the four signals into the APDs. The focusing length and multiplication factor of the glass-based focusing lens have been designed to be 600 μm and infinity, respectively. The total multiplication factor between the collimating lens and the focusing lens has been designed to be 2.5.

Instead of changing the optical path by 90° in the APD blocks [10], we have proposed to change the electrical signal path to increase the alignment tolerance and the coupling

Optics EXPRESS

efficiency [14]. For the perpendicularly electrical connection, the high speed electrical transmission lines are applied on the side wall of the ceramic submount for the APD attachment through analysis of signal integrity. The responsivity of each APD is typically 0.8 A/W when multiplication gain is 1. The input-referred noise density of the TIA is 10 pA/√Hz, and the 3-dB bandwidth of the TIA is typically 20 GHz. To guarantee the high-speed data transmission, we have developed the electrical connection structure of the flexible printed circuit board (PCB) [17].

3. Optical Investigation of the receptacle and the APD block

3.1 Performance of the receptacle and the APD block

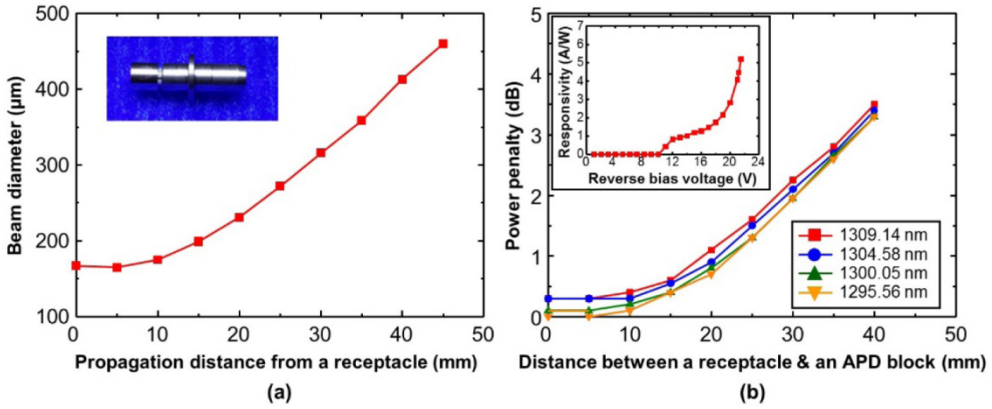

Fig. 2. (a) Optical beam diameter as a function of the propagation distance from a receptacle. (Inset: Fabricated receptacle.) (b) Power penalty as a function of the distance between a receptacle and an APD block. (Inset: Responsivity as a function of the reverse bias voltage of APD.)

The collimating lens inside the receptacle has been designed for the optical beam diameter to be less than 200 μm at the propagation distance of 15 mm from the receptacle [13]. The optical beam diameter after the optical signal propagation of 15 mm in air is estimated to be similar to the optical beam diameter of lane 0 at the APD block, which experiences the longest path in the TFF-based DMUX using the zigzag scheme, as shown in Fig. 1(c). In Fig. 2(a), the optical beam diameters have been measured as a function of the propagation distance from the receptacle by a beam profiler. The measured optical beam diameters are less than 200 μm at the propagation distance of 15 mm from the receptacle. The inset of Fig. 2(a) shows the fabricated receptacle.

In Fig. 2(b), the performance of the APD block has been measured as a function of the distance between the receptacle and the APD block. In the measurement, the 25.78-Gb/s non-return to zero (NRZ) optical signals were generated. The extinction ratios of the optical signals were set to be about 10 dB. The pattern lengths of the optical signals were 2^{31}–1. The inset of Fig. 2(b) shows the responsivity as a function of the reverse bias voltage in the APD. In the measurement, the reverse bias voltage was set to be 21.2 V for maximizing the receiver sensitivity of the APD block. The experiments were performed for the optical signals, which wavelengths were 1295.56 nm, 1300.05 nm, 1304.58 nm, and 1309.14 nm, to examine the wavelength dependence of the APD block. Those wavelengths were for lane 0, 1, 2, and 3 in Fig. 1(a), respectively. The power penalty was obtained for the bit error ratio (BER) of 10^{-9}. The baseline of the measurement was that the wavelength of the optical signal was 1295.56 nm and the distance between the receptacle and the APD block was 0 mm. In Fig. 2(b), the power penalties of the optical signals were less than 0.5 dB after the 15-mm propagation of the optical signal. As a result, the APD block could receive the optical signal within 0.5-dB

Optics EXPRESS

power penalty, if the beam diameter is less than 200 μm. There was the power penalty of about 0.2 dB between optical signals of different wavelengths due to the wavelength dependence of the APD's responsivity.

The optical beam diameters of four lanes have been also measured after a receptacle and a TFF-based DMUX for the examination of the optical coupling in the fabricated ROSA. The distance between the receptacle and a beam profiler was set to be 7 mm, which was determined by the distance between the receptacle and the APD block in the fabricated ROSA. The optical beam diameter of lane 0, 1, 2, and 3 were measured to be 195 μm, 179 μm, 181 μm, and 170 μm, respectively. Therefore, the APD block could receive four lanes within 0.5-dB power penalty in the fabricated ROSA without the insertion loss of the DMUX.

3.2 Alignment tolerance of the collimating lens in the receptacle

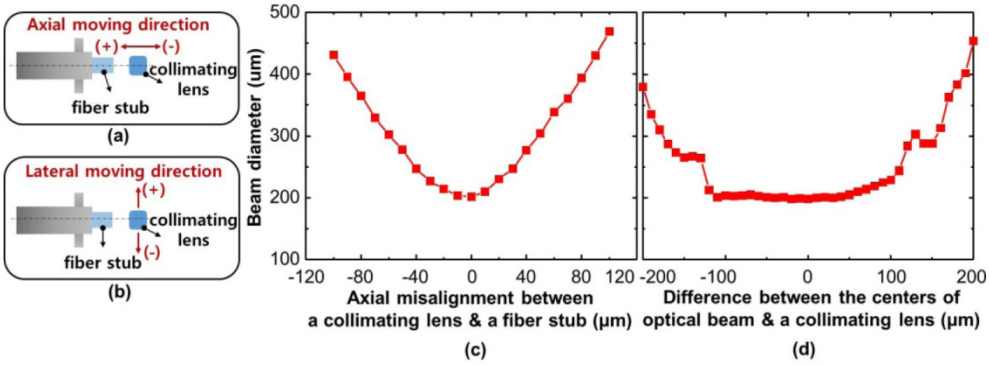

Fig. 3. (a) and (b) Experimental schematic for measuring the tolerance of the axial and the lateral misalignment between the fiber stub & the collimating lens, respectively. (c) and (d) Measurement of the optical beam diameters at the propagation distance of 15 mm from a collimating lens for the axial and the lateral misalignment between the fiber stub & the collimating lens, respectively.

The alignment tolerance between a fiber stub and a collimating lens in the receptacle has been experimentally investigated. Figures 3(a) and 3(b) show the experimental schematics to move the collimating lens for the axial misalignment between the fiber stub and the collimating lens and for the lateral misalignment between the centers of the fiber stub and the collimating lens, respectively.

In Fig. 3(c), the optical beam diameters have been measured at the propagation distance of 15 mm after the collimating lens as a function of the misalignment between the collimating lens and the fiber stub like Fig. 3(a). The position of 0 μm was defined that the collimating lens was set to be 700 μm, which was the focusing length, away from the fiber stub to maximize the coupling efficiency. The alignment tolerance was defined as the displacement of the collimating lens from the optimum position, where the beam diameter is increased by 10% (i.e. 0.5-dB power penalty has occurred, as shown in Fig. 2). The axial alignment tolerance between the fiber stub and the collimating lens is determined to be about ± 25 μm. In Fig. 3(d), the optical beam diameters have been also measured as a function of the difference between the centers of the fiber stub and the collimating lens like Fig. 3(b). The alignment tolerance of the displacement is observed to be from –120 μm to 100 μm. In the study's fabrication, the mechanical tolerance was estimated to be ± 5 μm. Thus, it is easy to passively align the collimating lens within the receptacle without performance degradation.

The lateral displacement in Fig. 3(b) could incur the small amount of the angular error in the output light of the receptacle. The average angular errors of the receptacles were measured to ~0.5°. The angular error might induce the error of the lane pitch of output light from TFF-based DMUX [7]. It was compensated by adopting the z-sleeve, as shown in Fig. 1(b), between the receptacle and the package and tilting the receptacle against the z-sleeve.

Optics EXPRESS

3.3 Alignment tolerance of the focusing lens in the APD block

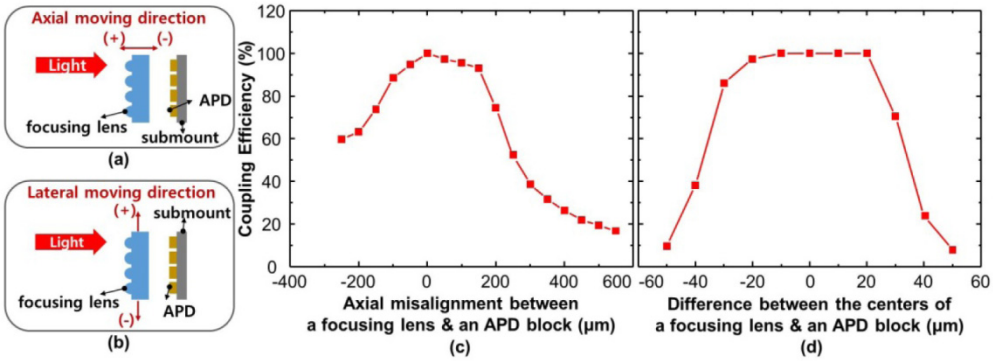

Fig. 4. (a) and (b) Experimental schematic for measuring the tolerance of the axial and the lateral misalignment between the focusing lens and the APD, respectively. (c) and (d) Measurement of the coupling efficiency of the APD for the axial and the lateral misalignment between the focusing lens and the APD, respectively.

In the APD blocks, it is also necessary to measure the alignment tolerance between the focusing lens and the APD. The focusing lens in the APD block has been designed to efficiently couple four optical signal into the APDs. Its focusing length has been designed to be 600 μm. The focusing lens of the APD block has been designed for the optical beam diameter at the focusing point to be less than 20 μm, because the diameter of the light sensitive area of the APD is 20 μm. Figure 4(a) and 4(b) show the experimental schematics to move the focusing lens for the axial misalignment and the lateral misalignment between the focusing lens and the APD, respectively. In the measurement, the wavelength of optical input signal was set to be 1295.56 nm. The reverse bias voltage to APD was set to 14 V. That is, the responsivity of APD was about 1 A/W. The power of the optical signal was –10 dBm. The distance between the receptacle and the focusing lens was set to be 15 mm. The beam diameter of optical signal at the focusing lens was estimated to be about 200 μm, as shown in Fig. 2(a). The coupling efficiency was defined as the ratio of the measured APD current to the maximum APD current. The position of 0 μm was defined that the focusing lens was set to be 600 μm, which was the focusing length, away from the submount to maximize the coupling efficiency. The alignment tolerance is also defined to be the displacement of the focusing lens from the optimum position, where the coupling efficiency is decreased by 10% (i.e. 0.5-dB penalty).

In Fig. 4(c), the coupling efficiencies have been measured, while changing the distance between the focusing lens and the APD like Fig. 4(a). The axial alignment tolerance between the focusing lens and the APD is determined to be from –100 μm to 150 μm. In Fig. 4(d), the coupling efficiencies have been also measured as a function of the difference between the centers of the focusing lens and the APD like Fig. 4(b). The alignment tolerance of the displacement was ± 25 μm. Thus, it is also easy to passively align the focusing lens in the APD block without affecting performance degradation.

4. Alignment tolerance of key components in the 4 × 25-Gb/s APD-ROSA

In the 4 × 25-Gb/s APD-ROSA with a TFF-based DMUX, there are three key components, which are a receptacle, a TFF-based DMUX, and an APD block. Figure 5 shows the structure of the fabricated 4 × 25-Gb/s APD-ROSA without a package. For the efficient fabrication, the alignment tolerances for all of the key components have been investigated. So the relative responsivities of four lanes in the APD block have been measured, while moving each key component in the directions of X-axis and Y-axis with fixing the other key components, as shown in Fig. 5. The reverse bias voltages to APD block were set to 15 V. That is, the

Optics EXPRESS

responsivity of APD block was about 1 A/W, considering the insertion loss of the TFF-based DMUX. The relative responsivity of each lane is defined as the ratio of the measured APD current to the maximum APD current of each lane. The optical power of each lane was set to be –10 dBm. The wavelengths of lane 0, 1, 2 and 3 were 1295.56 nm, 1300.05 nm, 1304.58 nm, and 1309.14 nm, respectively. The distance between the receptacle and the APD block was set to be 7 mm, which was determined by the size of the ROSA package. At the position of 0 μm, the relative responsivities of all lanes were maximized. The alignment tolerance is defined as the displacement of the key components from the optimum position, where the relative responsivity is decreased by 10% (i.e. 0.5-dB power penalty has occurred).

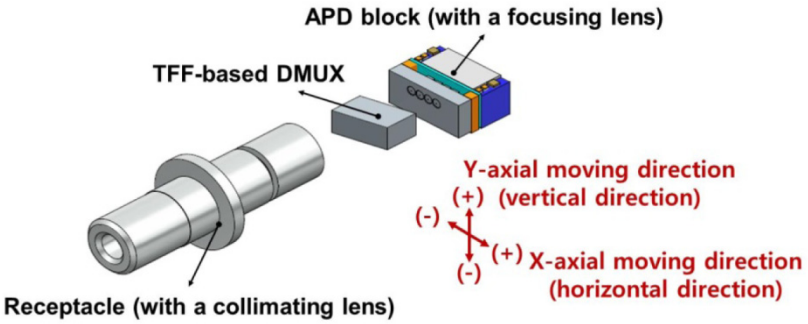

Fig. 5. Experimental schematic for measuring the alignment tolerance of a receptacle, a TFF-based DMUX and an APD block.

4.1 Alignment tolerance of the APD block

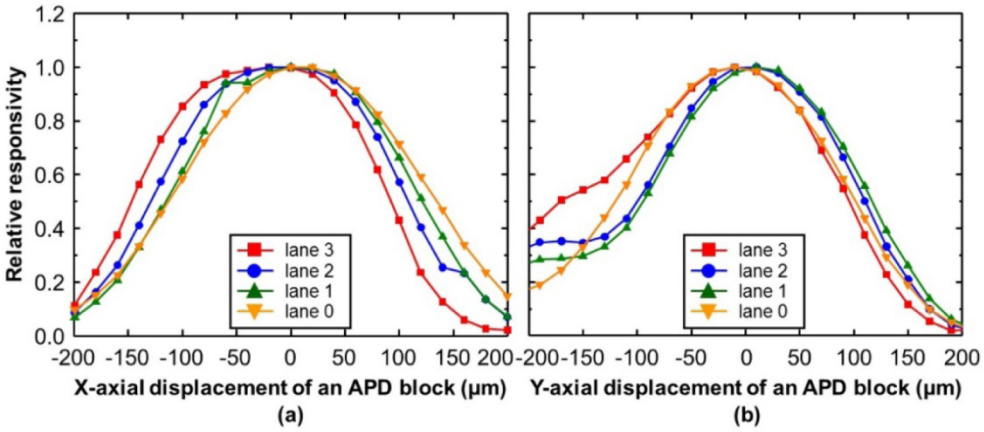

Fig. 6. Measurement of relative responsivities for four lanes while only moving the APD block in the direction of (a) X-axis and (b) Y-axis, with fixing the receptacle and the DMUX.

In Fig. 6(a), the relative responsivities of four lanes have been measured, while moving the APD block in the direction of X-axis with fixing the receptacle and the DMUX. The alignment tolerance of lane 0, 1, 2, and 3 are from –40 μm to 60 μm, from –60 μm to 60 μm, from –70 μm to 50 μm, and from –80 μm to 40 μm, respectively. The tolerance range of the lane 0 is smaller than the lane 1, 2 and 3 because the beam diameter of lane 0 is larger than any other lanes, as shown in Chapter 3. (The tolerance is determined by the diameter of the array lens, which has been designed to be 400 μm.) The centers of the alignment tolerance in lane 0 and 3 were different, because the pitch of four lanes is increased from 500 μm (designed) to 510 μm due to the error of the length in the DMUX [7]. The length of the DMUX was measured to 2.76 mm. The manufacturing error of the length was 60 μm

Optics EXPRESS

compared to the design value. Thus, considering all the lanes, the alignment tolerance is ± 40 μm for the X axial displacement of the APD block. If the dimension error of the DMUX can be reduced, the alignment tolerance can be improved to ± 60 μm.

Figure 6(b) shows the measurement of the relative responsivity for four lanes, while moving the APD block in the direction of Y-axis with fixing the receptacle and the DMUX. The alignment tolerance of lane 0, 1, 2, and 3 are from –60 μm to 40 μm, from –40 μm to 50 μm, from –40 μm to 50 μm, and from –60 μm to 40 μm, respectively. The centers of the alignment tolerances in lane 0 and 3 are different from those of lane 1 and 2. This is because there was the vertical angular error on the parallelism between the input region and the output region of the DMUX in Fig. 1. This non-parallelism also makes additional vertical angular errors on the output beams from the DMUX. These additional errors result in the asymmetry in the shape of the alignment tolerance. Thus, considering all the lanes, the alignment tolerance is also ± 40 μm for the Y-axial displacement of the APD block.

4.2 Alignment tolerance of the receptacle

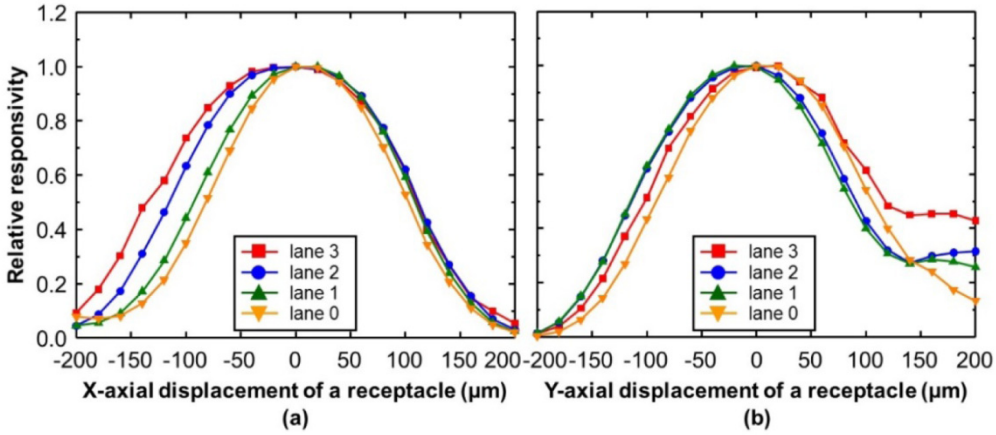

Fig. 7. Measurement of relative responsivity for four lanes while moving the receptacle in the direction of (a) X-axis and (b) Y-axis, with fixing the DMUX and the APD block.

In Fig. 7(a), the relative responsivities of four lanes have been measured, while moving the receptacle in the direction of X-axis with fixing the DMUX and the APD block. The alignment tolerance of lane 0, 1, 2, and 3 are from –30 μm to 50 μm, from –40 μm to 50 μm, from –60 μm to 60 μm, and from –70 μm to 50 μm, respectively. The tolerance range of the lane 0 is smaller than the lane 1, 2, and 3, because the beam diameter of the lane 0 is larger than any other lanes. The alignment tolerance of the receptacle is slightly smaller than the APD block. This is because the alignment tolerance of the receptacle is also limited by the dimension of the TFF-based DMUX, as shown in Fig. 1(c). The centers of the alignment tolerance in lane 0 and 3 were different because of the aforementioned manufacturing error of the length in the DMUX [7]. Thus, considering all the lanes, the alignment tolerance is from –30 μm to 50 μm (that is ± 40 μm) for the X-axial displacement of the receptacle.

Figure 7(b) shows the measurement of the relative responsivity for four lanes, while moving the receptacle in the direction of Y-axis with fixing the DMUX and the APD block. The alignment tolerance of lane 0, 1, 2, and 3 are from –30 μm to 50 μm, from –60 μm to 30 μm, from –50 μm to 40 μm, and from –40 μm to 50 μm, respectively. The tolerance range of the lane 0 is also slightly smaller than the lane 1, 2, and 3, because the beam diameter of the lane 0 is larger than any other lanes. The shape of the tolerance curves are also asymmetry because of the aforementioned additional vertical errors in the output beam angle due to the non-parallelism of the DMUX [7]. Thus, considering all the lanes, the alignment tolerance is ± 30 μm for the Y-axial displacement of the receptacle.

Optics EXPRESS

4.3 Alignment tolerance of the DMUX

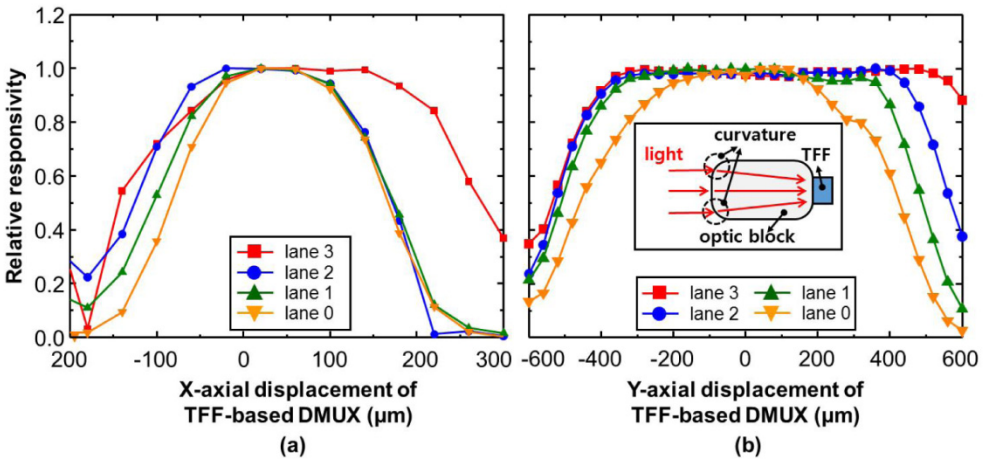

Fig. 8. Measurement of relative responsivity for four lanes while moving the DMUX in the direction of (a) X-axis and (b) Y-axis, with fixing the receptacle and the APD block. (Inset: Left side view of the DMUX, as shown in Fig. 1(c).)

In Fig. 8(a), the relative responsivities of four lanes have been measured, while moving the DMUX in the direction of X-axis with fixing the receptacle and the APD block. The alignment tolerance of lane 0, 1, 2, and 3 are from –30 μm to 110 μm, from –40 μm to 110 μm, from –70 μm to 110 μm, and from –40 μm to 200 μm, respectively. The tolerance range of the lane 3 is much larger than the lane 0, 1 and 2, because the light path of lane 3 inside the DMUX is not affected by the HR coating region, as shown in in Fig. 1(c). The tolerance range of the lane 0 is smaller than the lane 1, 2 and 3, because the beam diameter of lane 0 is larger than any other lanes, as shown in Chapter 3. Thus, considering all the lanes, the alignment tolerance is from –30 μm to 110 μm (i.e. ± 70 μm) for the X-axial displacement of the DMUX. The tolerance is determined by the width of each TFF in the DMUX. The width of the TFF is 500 μm and its effective width is 400 μm. The alignment tolerance is additionally limited by the aforementioned error of the lane pitch due to the manufacturing error of the DMUX length [7].

Figure 8(b) shows the measurement of the relative responsivity for four lanes, while moving the DMUX in the direction of Y-axis with fixing the receptacle and the APD block. The alignment tolerance of lane 0, 1, 2, and 3 are from –260 μm to 220 μm, from –380 μm to 380 μm, from –400 μm to 460 μm, and from –400 μm to 580 μm, respectively. It is noted that the alignment tolerance of the lane 1, 2, 3 is much larger than the length of the TFF. This is because the input light was refracted at the curvature of the molded optic block of the DMUX like the inset of the Fig. 8(b). The curvatures are formed by the molding process. The alignment tolerance of lane 0 is decreased compared to other channels because of the aforementioned additional vertical angular errors on the output beams due to the non-parallelism of the DMUX. Thus, considering all the lanes, the large alignment tolerance is obtained to be from –260 μm to 220 μm (i.e. ± 240 μm) for the Y-axial displacement of the DMUX.

In the investigation, the alignment tolerance of the DMUX was much larger than other key components such as the receptacle and the APD block. So, in the fabrication of the ROSA, the receptacle and the APD block have first been assembled to maximize the performance of the ROSA. Although the horizontal and vertical angular errors can be occurred during the assembly process, it can be suppressed by properly rotating the DMUX in the opposite direction of the angular error.

Optics EXPRESS

5. Performance of the 4 × 25-Gb/s ROSA

Figure 9(a) shows the fabricated ROSA. The body size is 10.65 x 6.6 x 5.6 mm^3 (L x W x H) without the receptacle and flexible PCBs. It is very compact to be applied in a CFP4 transceiver or a QSFP28 transceiver [11]- [12]. Figure 9(b) shows the relative responsivity as function of the wavelength of the each lane. The 0.5-dB bandwidths of four lanes are observed to be larger than 3 nm. In the measurement, the reverse bias voltages of APDs were set to 15 V, thus multiplication gain was approximately 1.4. That is, the responsivities of APDs were about 1 A/W, considering the insertion loss of the DMUX. Optical input power of each lane was set to be –10 dBm. The output current of each APD has been measured while changing the wavelength of the optical input signal. The responsivities of lane 0, 1, 2, and 3 were observed as 0.95 A/W, 1.01 A/W, 1.01 A/W, and 0.99 A/W, respectively, at the center wavelengths of four lanes. The total insertion loss, including the DMUX loss and the coupling loss, could be estimated to be about 0.5-0.8 dB, considering the responsivities and multiplication gains of the APDs.

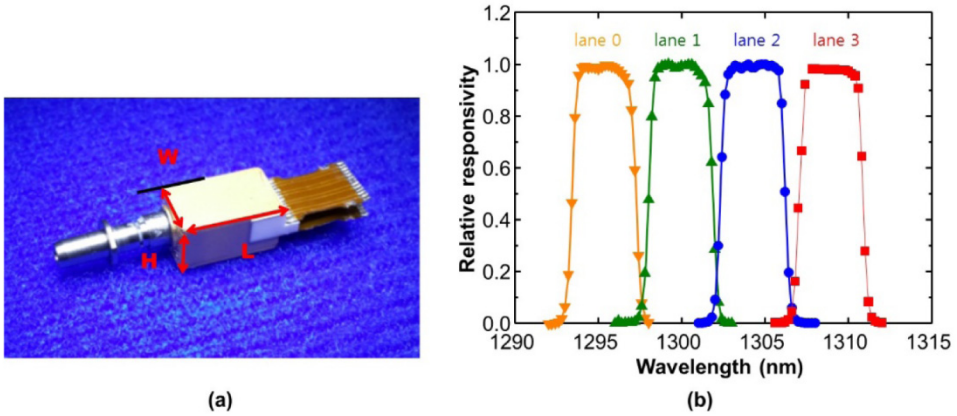

Fig. 9. (a) Prototype of the 4 × 25-Gbps APD-ROSA. (b) Optical bandwidth of the 4 × 25-Gbps APD-ROSA.

Figure 10 shows the performance of the 4 × 25-Gbps APD-ROSA. In the measurement, the 25.78-Gb/s optical NRZ signals were obtained by using a $LiNbO_3$ Mach-Zehnder intensity modulator. The extinction ratios of optical signals were set to be about 10 dB. The pattern length was 2^{31}–1. The wavelengths of lane 0, 1, 2 and 3 were 1295.56 nm, 1300.05 nm, 1304.58 nm, and 1309.14 nm, respectively. The BERs of all lanes in the ROSA have been measured at back-to-back link and after 60-km SSMF transmission. The reverse bias voltages of APDs were set to be 21.2 V, where multiplication factors of APDs were about 6, to achieve the minimum receiver sensitivity. The receiver sensitivities of lane 0, 1, 2, and 3 are measured to be –22.4 dBm, –22.7 dBm, –22.7 dBm, and –22.2 dBm (at the BER of 10^{-12}), respectively, in Fig. 10(a). It is the best performance, to our knowledge, despite the lower multiplication factors of the APDs [3, 4, 18]. The receiver sensitivity of lane 3 is worse than lane 1 and 2, because of the wavelength dependence of APD, as shown in Fig. 2(b). And, the performance of lane 0 is worse than lane 1 and 2. This is because the lane 0 experiences longer path than any other lanes. As a result, the power penalty occurred due to the coupling loss, as shown in Fig. 2(b), and the insertion loss of the DMUX. The error free operation has successfully been demonstrated after 60-km SSMF transmission. The loss of the 60-km SSMF fiber was 19.8 dB. After transmission, the power penalties were 0.1-0.2 dB caused by the chromatic dispersion of the fiber. Figure 10(b) shows the measurement of eye diagrams at back-to-back operation when the power of each lane was set to be –20 dBm.

Optics EXPRESS

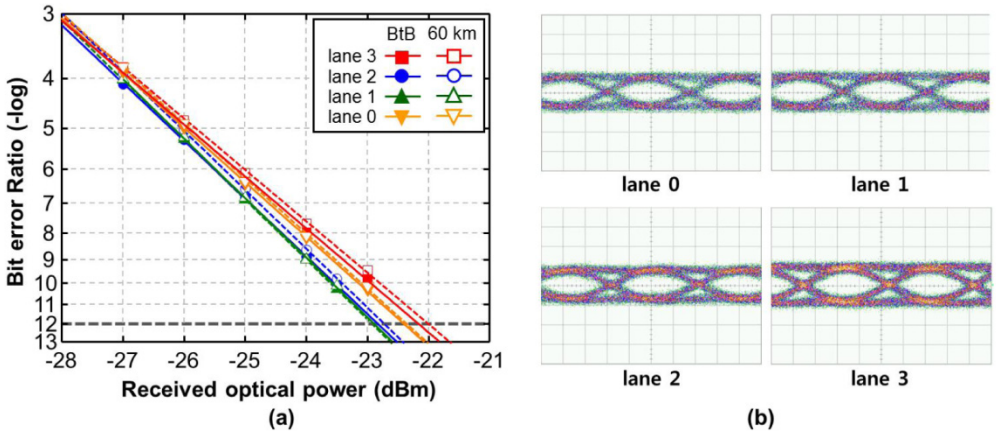

Fig. 10. (a) Performance of the ROSA at back-to-back link and 60-km SSMF transmission. (b) Measurement of electrical eye diagrams with the ROSA for four lanes in back-to-back link, when the optical power of each lane was –20 dBm.

6. Summary

In this paper, we have investigated and developed the performance of the highly alignment tolerant and high-sensitivity 100-Gbps (4 × 25-Gbps) APD-ROSA with the TFF-based DMUX. The experimental investigation shows that the collimating lens and the focusing lens in the receptacle and the APD block, respectively, could be passively assembled because the alignment tolerance is larger than ± 25 μm. We have also investigated the alignment tolerance of the key components such as the receptacle, the TFF-based DMUX and the APD block. The alignment tolerances for the X-axial displacement have been measure to be ± 40 μm, ± 70 μm, and ± 40 μm, respectively. In case of the Y-axial displacement, the alignment tolerances have been determined to be ± 30 μm, ± 240 μm, and ± 40 μm, respectively. In addition, it is possible to improve the alignment tolerance by reducing the dimensional error of the DMUX block. We have also measured the receiver sensitivities of lane 0, 1, 2 and 3 for the 25.78-Gb/s NRZ signals to be –22.4 dBm, –22.7 dBm, –22.7 dBm, and –22.2 dBm (at the BER of 10^{-12}), respectively, in the back-to-back link. These were the best performance, to our knowledge, despite the low multiplication factor of the APDs. In addition, we have successfully demonstrated the error free operation for the 60-km SSMF transmission

Funding

This work was supported by Institute for Information & communications Technology Promotion (IITP) grant funded by the Korea government (MSIP) (No.B0101-16-0024, Terabit optical-circuit-packet converged switching system technology development for the next-generation optical transport network).